Toward the Future Generation of Railway Localization Exploiting RTK and GNSS

Towards the Future Generation of Railway Localization Exploiting RTK and GNSS

Denis Mikhaylov, Carla Amatetti, *Student Member*, IEEE, Tommaso Polonelli, *Member*, IEEE, Enea Masina, Riccardo Campana, *Student Member*, IEEE, Kai Berszin, Charles Moatti, Davide Amato, Alessandro Vanelli-Coralli, *Senior Member*, IEEE, Michele Magno, *Senior Member*, IEEE, Luca Benini, *Fellow*, IEEE

***Abstract*—Smart sensors have become pervasive in railway transportation applications, particularly in Europe where digital technologies are increasingly being applied to the railway signalling field. In the future, safety-critical track-side train detection equipment, such as track circuits and axle counters, will be eliminated in favor of an accurate position estimate supplied by the train. However, the best approach to calculate an accurate position estimate remains an open research question, especially due to the high availability and reliability required. This paper describes two static experiments performed with a GNSS module, which demonstrate that the real-world accuracy achievable with GNSS and Real Time Kinematic (RTK) alone is not sufficient for safety-critical applications, meaning further complementary sensors are required. Furthermore, a custom sensor node containing a GNSS module with RTK and an Inertial Measurement Unit (IMU) has been used to acquire several data sets from an operating passenger train during dynamic tests on a railway line between Formigine and Modena, in Emilia-Romagna, Italy. These labeled GNSS and IMU data have been made freely available to the scientific community. The positioning accuracy of the GNSS and RTK measurements is evaluated, providing an in-depth study of the localization error and satellite coverage on the entire route. We demonstrate, with experimental evaluation, that centimeter accuracy (1.9 ± 0.8 cm) is achievable under favorable static conditions, while accuracy can deteriorate to 8 m with RTK in urban scenarios with many reflections and poor sky view, worse than with GNSS alone. Under controlled conditions we show that shielding the GNSS receiver without RTK with a grounded metal plate causes a reduction in accuracy from 0.80 ± 0.04 m to 3.70 ± 0.55 m in the least and most shielded case respectively. Our dynamic tests on a train show that although at least meter-level accuracy (1.08 ± 1.30 m) is achievable with GNSS and RTK alone under dynamic conditions, a sensor fusion approach is necessary to accurately localize trains when GNSS conditions are poor or GNSS is unavailable.**

***Index Terms*—Railway, GNSS, Network RTK, IMU, Smart Rail, ETCS, ERTMS, Sensor Fusion**

I. Introduction

THE European railway sector is currently on the brink of a revolution which aims to create a common standard for railway signalling and to enhance cross-border interoperability [1]. All elements of the railway system, including the railway infrastructure subsystem and Traffic Management System, must be modernized in terms of reliability, capacity, and costs [2]. In Europe in particular, there is a need for standardization of these systems, in order to interconnect the numerous country-specific and often incompatible systems currently in use, to allow international trains to run more seamlessly, and to reduce costs by applying economies of scale. Furthermore, tracking the position of trains is also needed for other, non-safety-critical applications, e.g. passenger information and fleet management.

Current railway signalling systems almost universally require track-based train detection systems such as track circuits or axle counters [3], which are expensive to install and maintain and pose inherent safety risks to those doing so due to their location. In future, an entirely train-based localization system is envisioned, removing the need for infrastructure-based train detection systems, as part of the future European Rail Traffic Management System (ERTMS) and European Train Control System (ETCS) Level 3. However, this requires on-train positioning technology which provides centimeter-level position accuracy, while applying *Reliability, Availability, Maintainability and Safety* principles and enabling safety-critical certification [1].

Today, a common way of providing globally referenced positioning in integrated navigation systems is the Global Navigation Satellite System (GNSS) [4]. Although stand-alone GNSS would minimize costs, its use in the railway sector is still limited [5], as the accuracy provided of around 1-3 m is not sufficient for safety-critical applications. Thus, for such applications, more sophisticated algorithms based on differential position, such as the Real Time Kinematic (RTK), or absolute position, e.g. Precise Point Positioning (PPP), are needed [6]. However, due to the absence or distortion of GNSS signal in tunnels and under trees, as well as due to local effects such as multi-path or spoofing, it is not always possible to guarantee an acceptable navigation accuracy and reliability even when these techniques are applied.

Therefore, to enhance the robustness, effectiveness, and security of GNSS-based train localization systems, several integrated positioning solutions have been proposed [7]–[10]. One approach is to combine localization results provided by an Inertial Navigation Systems (INS) and the GNSS, with the aim to detect a GNSS signal fault during long signal outages and to improve the reliability of the obtained position by means of redundant measurement data from onboard sensors [11]. However, designing a wireless sensor node compliant with the

Denis Mikhaylov, Tommaso Polonelli, Enea Masina, Kai Berszin, Charles Moatti, Michele Magno, and Luca Benini are with D-ITET department ETH Zürich, Zürich, Switzerland (e-mail:{mdenis, topolonelli, masinae, kberszin, cmoatti, magnom, lbenini}@ethz.ch

Carla Amatetti, Riccardo Campana, and Alessandro Vanelli-Coralli are with DEI, University of Bologna, Bologna, Italy (email: {carla.amatetti2, riccardo.campana7, alessandro.vanelli}@unibo.it

David Amato is with Sadel S.p.A, Bologna, Italy (e-mail: davide.amato@sadel.it

rigorous safety-critical positioning requirements in the severe propagation environment typical for the railway sector still presents a challenge, and such devices are not yet available on the market [12]. Although commercial solutions for sensor fusion of GNSS and an IMU exist for other applications, the algorithms used are generally proprietary and not easily modifiable by the user. They are also not optimized for railway applications.

This work extends the conference paper [13] which presented a low power custom multi-sensor wireless node designed to investigate the feasibility of localizing trains with centimeter accuracy using GNSS with RTK and inertial sensors. In this paper, we evaluate the GNSS and RTK performance of the sensor node on-board a passenger train on a real railway line in Emilia-Romagna, Italy, generating the first data set of this kind to be made freely available as open data, for future work by academic and industry researchers[1]. By collecting and publishing raw IMU and GNSS+RTK position data, we aim to make it easier for novel sensor fusion algorithms for railway applications to be developed and evaluated in the future. In this work, we analyze the effect of antenna position within the train on GNSS and RTK positioning performance, including the number of satellite signals received and the error in the calculated position based on a ground truth. We demonstrate the need for the inertial sensors in situations where GNSS is not available, such as tunnels or highway underpasses. To provide a baseline for our on-train dynamic tests, we also present two static tests which quantitatively evaluate the achievable accuracy of the GNSS when the antenna sky view is shielded (as would be the case inside a train). It should be noted that this paper reuses some technical content from theses [14] and [15] with permission.

To summarize, this paper offers the following novel contributions:

- Quantitative investigation evaluating RTK performance under various real-world static sky view environments, assessing its limitations in the context of railway environments
- Quantitative investigation of the effect of antenna shielding on GNSS positioning accuracy
- A new open data set containing GNSS+RTK and IMU data from dynamic tests on a real passenger train, which can be used for the development of novel sensor fusion approaches in future.
- Analysis of the satellite coverage and GNSS+RTK accuracy on a measurement run from the new open data set

Section II describes the state of the art and provides some background on GNSS and RTK. Section III describes the custom sensor node used during the dynamic tests for data collection. Section IV describes the static tests performed to evaluate the performance of RTK and GNSS under various sky view conditions and the effect of obstructing the sky view (e.g. due to a train cab windscreen). Section V describes the dynamic tests performed on a railway line between Formigine and Modena in Emilia-Romagna, Italy. Section VI concludes the work.

[1] github.com/ETH-PBL/Railway-Precise-Localization

II. Related works and Background

Localization is an increasingly important research topic in a wide range of fields. GNSS technology therefore continues to develop to better match the requirements of various applications, which are summarized in [10]. The rail industry has its own use cases and requirements for GNSS-based systems which are described in [5]. They distinguish between safety-critical applications, such as absolute positioning for ERTMS systems or track worker protection, and so-called liability-critical applications, such as surveying, condition monitoring or cargo wagon tracking, where positioning information could be used to determine liability, but is not safety-critical. There are also applications, such as on-train reservations, that are neither safety- nor liability-critical [5].

A particular problem with GNSS is proving its integrity and reliability in unfavorable conditions. Recent literature has presented numerous solutions to handle various aspects of the degradation caused by local phenomena using detection and mitigation techniques [16]–[18]. Multi-path and/or Non-Line-of Sight (NLOS) mitigation is a mature field of research [19]–[21]. However, research continues on the potential applications and behavior of RTK. For example, in [22], the authors analyze the deviation of the expected and observed pseudorange of the reference station in the RTK and N-RTK algorithms, to increase the reliability of these techniques in railway applications.

The suitability of GNSS systems for railway applications has also been investigated and evaluated through field tests and proofs of concept as part of numerous funded projects. SATLOC-2[2], ERSAT-EAV[3], 3InSat[4], and GaLoROI[5] developed and validated the use of GNSS in train localization at signalling system level and showed that the use of complementary positioning techniques is essential. The objective of X2RAIL-4[6] and X2RAIL-5[7] is to enhance performance at a railway system level by introducing new functionalities that enable and develop future signalling and automation concepts by relying on the use of GNSS, at a European level.

GNSS sensor fusion is also not a new topic, particularly with the use of an IMU [7]. Other types of sensors such as barometers and magnetometers have been evaluated on trains, but were found to perform poorly [11]. Localization approaches based on identifying specific track features have also been evaluated and found to show potential, including track irregularity matching [8], and LiDaR in tunnels [23]. For railway surveying and maintenance applications, smaller-scale localization techniques have also been applied to measure track geometry [24]. Thanks to their complementary properties, GNSS and IMUs can be integrated so to improve the accuracy and robustness of localization [7], [9]. Sensor fusion of GNSS

[2] https://uic.org/projects/article/satloc-2
[3] www.ersat-eav.eu
[4] https://business.esa.int/projects/3insat
[5] www.galoroi.eu
[6] https://projects.shift2rail.org/s2r_ip2_n.aspx?p=X2RAIL-4
[7] https://projects.shift2rail.org/s2r_ip2_n.aspx?p=X2RAIL-5

and IMUs has been shown to achieve measurement errors of less than $0.6\,\mathrm{cm}$ and $1.1\,\mathrm{cm}$ in the horizontal and vertical directions respectively, when GNSS reception is uninterrupted along the railway line [7]. Nevertheless, establishing the accuracy of the localization solution provided by an on-board GNSS-based system remains a challenging issue due to the varying environment in which trains operate. Therefore, the positioning performance in the railway sector must be evaluated in different operating conditions. A survey by Otegui et al [25] describes and compares tests and simulations from the literature performed using GNSS and IMU in a railway context. They conclude that the combination of a GNSS module and a MEMS IMU is the most promising from an commercial viability and performance perspective, but identify a lack of research specifically into safety-critical applications of this approach, limited experimental data from field tests, and challenges in finding a reliable ground truth with which experimental data can be compared. A quantitative specification of the localization accuracy and frequency that is desirable in railway applications is provided in [26], namely a position accuracy of within $10\,\mathrm{m}$ every $5\,\mathrm{s}$ in the longitudinal track direction, together with correct track identification which requires much higher positioning accuracy.

Validation of the numerous localization approaches proposed in the literature remains a challenge, although some successful simulation frameworks have also been developed for some types of sensors [27]. Unlike for other types of vehicles, there are, to the authors' knowledge, no open data sets of IMU, GNSS and RTK from on-board a train. The data collected for this work will therefore be made available for this purpose. Similarly, there does not appear to be any proven sensor fusion algorithm that can be applied out of the box. This work aims to contribute to the former problem, paving the way for future publications on the latter subject.

Background: GNSS, RTK and N-RTK

GNSS allows the absolute position, velocity, and time (PVT) of an object to be calculated with an accuracy of approximately 1-$3\,\mathrm{m}$ under ideal conditions. The GNSS receiver computes its position based on signals coming from multiple GNSS satellites, which are on orbits around $20\,000\,\mathrm{km}$ away from Earth. The receiver location is obtained by solving the *pseudoranges* (ρ), which define the measure of the time needed to travel from a satellite to the receiver, and the *carrier phase* (ψ), which expresses a measure of the distance between satellite and receiver in terms of units of cycles of the carrier frequency. However, both are biased measurements of the distance.

Numerous types of errors degrade the PVT solution obtained by the GNSS receiver and can be broadly described as follows: *(i)* control system errors, including ephemeris errors, on board and receiver clock biases; *(ii)* atmospheric errors due to the Ionosphere and Troposphere. In particular, in the Ionosphere region, the propagation speed of the signal depends on the number of free electrons along the path, which induces a delay in both the phase measurement and pseudorange calculation. This kind of error can be compensated through a multi-band receiver, enabling an accuracy of $1\,\mathrm{m}$ to be achieved. After passing the Ionosphere, the signal enters the Troposphere, where dry air and water vapor additionally delay the carrier signal; *(iii)* Finally, there are reception errors, which include multi-path, receiver antenna bias, equipment delays, and thermal noise.

Standalone GNSS cannot provide centimeter-level accuracy due to the errors described above. Therefore, to increase accuracy, more sophisticated algorithms have been developed which require additional inputs compared to GNSS alone. Real Time Kinematic (RTK) is a technique used to improve the quality of the GNSS position estimates. RTK-capable GNSS receivers take standard GNSS satellite signals as input along with a ground-based correction stream to achieve centimeter-level positional accuracy. The RTK system consists of a user and one or more reference stations. These reference stations, located at a known position, measure pseudoranges by receiving signals from the satellites in view. By comparing the estimated position in real time with the known ground truth, the reference station can compute measurement correction messages, which are broadcast to the users. This technique exploits the high correlation in space and in time of the GNSS error sources described above, in particular of the atmospheric errors. However, the accuracy improvement is heavily constrained by the distance between the receiver and base station and decreases as distance increases. For centimeter-level performance, the maximum distance is around 10-$15\,\mathrm{km}$ [28]. To overcome this limitation, an enhancement of the RTK, named Network RTK (N-RTK), has been developed. In N-RTK multiple reference stations share their corrections with a server, which, in turn, forwards them to the users through the Networked Transport of RTCM via Internet Protocol (NTRIP).

One of the most common techniques employed by N-RTK is the Virtual Reference Station (VRS) method [29]. This algorithm aims to minimize the gap between the receiver and the reference station by generating a VRS close to the user position which combines data from multiple physical reference stations around the user. In this way, the spatially and temporally correlated errors can be eliminated. The position of the VRS is computed based on the raw GNSS user position, and sent to the server using a standard National Marine Electronics Association (NMEA) message as part of the NTRIP protocol. Thus, N-RTK requires bi-directional communication between the user and the server. As the distance between the user and the VRS location increases, the provided solution degrades. Therefore, a new VRS needs to be generated, which usually cannot be done in real-time.

The solutions provided by a GNSS module using RTK are of three types: *(i) Stand-alone* mode, *(ii) Fix* mode, and *(iii) Float* mode. The former works without corrections, delivering the same positioning solution as with stand-alone GNSS. In *Fix* mode, the receiver is able to solve the ambiguity of the carrier phase. This mode reports the ambiguity as integer value, meaning that the position has been determined; finally, *Float* mode provides the carrier phase as a floating number, meaning the RTK is active but is unable to determine the precise position [30]. While RTK is now standard in surveying applications, its use in the railway sector is limited

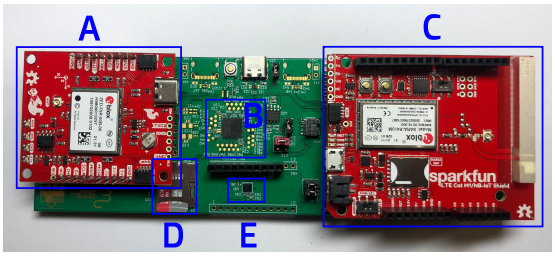

Fig. 1. Overview of the custom localization sensor node where: (A) ZED-F9P GNSS module, (B) STM32L452CEU MCU, (C) SARA-R410M cellular module, (D) microSD card, (E) ASM330LHH IMU

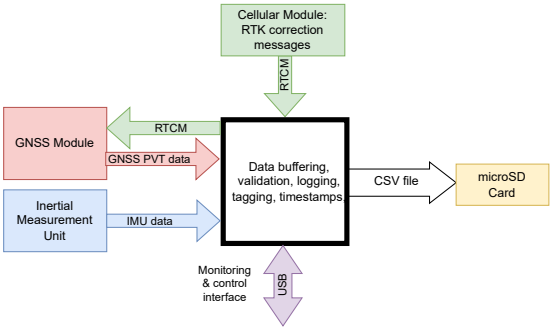

Fig. 2. Overview of the data flows in the sensor node during logging.

so far to infrastructure maintenance tasks [31] and increasingly for maintenance worker tracking and geofencing [32]. Its feasibility for safety-critical train positioning has yet to be extensively investigated in practice. Such an investigation is performed in this work.

III. Hardware Sensor Node for Data Collection

To perform the dynamic tests described in this paper, a custom low power sensor node was developed to collect, validate, and store position and inertial measurements with precise timestamps in the order they are received. It consists of an STM32L4 (STM32L452CEU) Microcontroller Unit (MCU) with an ARM-Cortex-M4F core, an ASM330LHH IMU, a microSD card slot for local data storage, a u-blox ZED F9 GNSS module, and a NB-IoT (Narrowband IoT) SARA-R410M module. The node is depicted in Fig. 1.

A. Functional Overview

An overview of the sensor node behavior during data collection is given in Fig. 2. The data from the GNSS module and IMU are received by the MCU, which validates each data measurement and buffers it. The buffered data is then written to an SD card using the CSV file format, with each line containing a timestamp obtained from the internal Real-Time Clock (RTC), a tag indicating the data type (U for UBX, N for NMEA and I for IMU data), followed by the payload of UBX, NMEA, or IMU data. RTK correction messages in RTCM format are received by the MCU via the cellular module, which forwards them directly to the GNSS module to be used when calculating a positioning solution. A monitoring and control interface via USB-C allows data logging to be started and stopped, and for some summary data such as number of satellites in view or current position to be seen in real time during data logging. In addition, the same interface can be used to manually incorporate timestamped and synchronized comments and labels in the final CSV file together with the stored sensor data, as can be seen in Section V, where the plots are labeled with the arrival and departure time at each railway station. Additional labels are also stored automatically whenever the state of the cellular connection with the RTK corrections changes. Currently, no processing or sensor fusion is performed on the sensor node itself.

B. Choice of Hardware and Technical Implementation

The STM32L4 MCU was selected due to its low cost and its ease of programming for prototyping purposes. It is sufficiently powerful to buffer and log the sensor data, and has a Real-Time-Clock allowing timestamps with sub-millisecond precision. It is also able to manage the communication with the cellular module.

The ASM330LHH from ST is a low-cost 6-axis automotive MEMS IMU offering synchronized output on all axes at high frequency. The IMU data was recorded at $1667\,\mathrm{Hz}$ with measurement ranges of $\pm 2\,\mathrm{g}$ and $\pm 125\,\mathrm{dps}$ for the accelerometer and gyroscope respectively. In this configuration the manufacturer promises sensitivities of $0.061\,\mathrm{mg/LSB}$ and $4.37\,\mathrm{mdps/LSB}$ respectively, with a sensitivity tolerance of $\pm 5\,\%$ and a cross-axis sensitivity of $\pm 1\,\%$ for both accelerometer and gyroscope measurements. The typical angular random walk is given as $0.21\,\mathrm{deg}/\sqrt{\mathrm{h}}$ with a bias instability of $3\,\mathrm{deg/h}$.

The SARA-R410M module is used to receive the RTK correction packets via a cellular connection from two, easily configurable remote sources. The sensor node can establish a connection to a commercial public NTRIP server. Alternatively, a direct connection to a raw TCP socket can be used instead, to receive corrections from a custom base station consisting of another GNSS module. Support for VRS in the NTRIP case was not implemented, as it was not needed for the tests, but can be easily added if required. To detect and rectify connection loss, a simple watchdog timer on the MCU restarts the SARA module whenever the last RTK packet was received more then $10\,\mathrm{s}$ ago, thus resetting the cellular connection.

To achieve the most accurate localization in all possible use cases, a multi-band GNSS module implementing RTK is required. For this reason, among different commercial solutions, the ZED platform from u-blox was chosen. This module can combine the signal from multiple GNSS constellations to achieve precise and robust positioning and, as shown in previous in-field investigation [13], provides sub-meter precision in static and dynamic conditions. Another feature of the ZED family is the native support for the RTCM protocol allowing easy integration with the aforementioned cellular setup. The ZED-F9P and ZED-F9R are the two variants selected from the ZED family, where the F9P model can work both as a RTK base station or a RTK rover. This feature gives the flexibility to build a private RTK network without relying on commercial RTK-NTRIP servers. Both variants promise $1.5\,\mathrm{m}$ accuracy

with GNSS alone and 1 cm accuracy with RTK corrections. In each of the tests described below, the module was configured to output UBX-NAV-PVT messages at a frequency of 1 Hz.

During the data logging, the sensor node without the SARA-R4 module has an average power consumption of 673 mW. With the cellular interface enabled, the average power is up to 1 W, which is negligible in a railway context.

IV. Static Tests

To evaluate the performance of the sensor node with GNSS and RTK under static conditions, two different tests were performed. Firstly, the GNSS module was evaluated under various real-world sky view conditions with and without RTK. Subsequently, to quantify the possible effect of the train cab on the sky view of the GNSS, a test was performed using a metal plate to shield a specific portion of the sky view.

A. GNSS and RTK in Real Environments

The static tests were performed in different propagation environments, i.e., rural, suburban, and urban, to quantify the accuracy under Line-of-Sight (LoS) and Non-Line-of-Sight (NLoS) conditions both when RTK is enabled and when it is not.

Method: To precisely evaluate the accuracy of the GNSS module in a static setup, we used the geodetic points from the Federal Office of Topography Swisstopo and the Stadt Zürich - Tiefbau - und Entsorgungsdepartement - Geomatik + Vermessung. These points are bolts or stones that mark fixed points with 3 cm precision. For each measurement, the ZED-F9P module was placed on a geodetic point, turned on (cold start), and allowed to acquire signal for five minutes without recording. Afterwards, the position measurements were recorded for a further 5 minutes with a sampling rate of 1 Hz. The measurements were acquired in four different, increasingly obstructed environments, with and without RTK correction. The positioning error is calculated by comparing the known position of the geodetic point to the position reported by the GNSS module. The swipos-GIS/GEO from Swiss Positioning Service swipos is used as the RTK network. It provides RTK correction data from 31 AGNES (Automated GNSS Network for Switzerland) base stations which use GNSS signals from all four satellite constellations. Although swipos also offers VRS endpoints using NTRIP, only fixed AGNES stations were used in this test, as this reduced complexity and the distance to the nearest base station was very small (less than 5 km).

Results: Fig. 3a reports the localization precision without RTK, and Fig. 3b reports RTK measurements. The 25$^{\text{th}}$ and 75$^{\text{th}}$ percentile range are represented by the upper and lower boundary of each box. The red lines indicate the median value of the measurements. Table I shows a summary of the experimental statistics for these static tests, where it can be seen that the error standard deviation is reduced by a factor of 10 when the RTK is enabled. Moreover, the mean error is reduced by more than 1 m while using RTK in an open environment. With RTK enabled, in the urban and alley environments, the error is 5 m and 8 m respectively, compared to 2.5 m, and 4.9 m without RTK. This error comes from

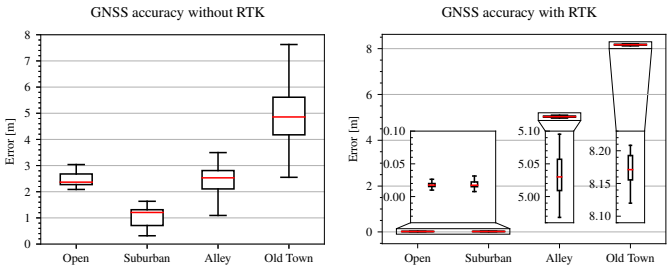

Fig. 3. (a) Box plot of static measurement accuracy without RTK, (b) Box plot of static measurement accuracy with RTK, with magnified sections on measurements to illustrate the small variance with a large mean error

TABLE I
Localization accuracy for static tests with and without RTK

Metrics		Rural	Suburban	Alley	Urban
μ (m)	RTK off	2.465	1.0675	2.475	4.897
	RTK on	0.019	0.019	5.0349	8.1719
σ (m)	RTK off	0.237	0.354	0.595	1.353
	RTK on	0.008	0.005	0.033	0.022

the multi-path distortion of the GNSS signal, which degrades the accuracy of RTK. In addition, these error sources are uncorrelated with the RTK base station, and result in a total error equivalent to the sum of the multi-path error variance of each base station alone [33].

Conclusion: We conclude that RTK is necessary in order to achieve a variance of less than 35 cm, as required for railway localization applications. However, RTK is not the solution to all GNSS accuracy problems. The alley and urban experiment locations demonstrate that even an accurate measurement can suffer from a large offset error due to the multi-path effect. In order to detect and mitigate this kind of error complementary sensors need to be used.

B. GNSS with a Shielded Antenna

Further, we evaluated the possible effect of shielding the GNSS antenna, for example due to the train cab, on the positioning accuracy.

Method: The test was performed using a ZED-F9P module and a TOPGNSS TOP106 L1/L2 multi-band antenna, shielded with a grounded metal plate. This plate can rotate along its lower edge, positioned near the antenna mounting point. In this way, it is possible to fix the shield at selected angles with respect to the ground. The shield can be set from a vertical position (90°), with minimum effect on the antenna, up to an horizontal position (0°), with maximum shielding effect. The setup is shown in Fig. 4a.

For each measurement, the ZED-F9P module was turned on (cold start), and allowed to acquire signal for five minutes without recording. Afterwards, the position measurements were recorded for a further 5 minutes with a sampling rate of 1 Hz. The test was performed with 90, 70, 60, 40, and 20 degrees of shielding angle without RTK. The positioning error is calculated by comparing the known position of the geodetic point to the position reported by the GNSS module.

(a)

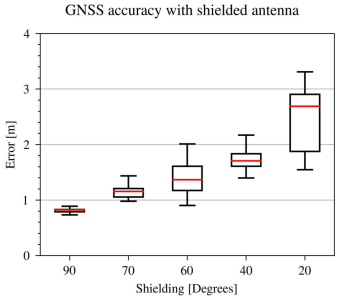

(b)

Fig. 4. Static antenna shielding test setup (a) and results as box plot showing static measurement accuracy without RTK at different angles (b)

Results: The positioning accuracy is shown in Fig. 4b, where the results show that decreasing the angle of shielding decreases the positioning accuracy and increases the variance of the measurements. For example, we can consider the two extreme cases of (90°) and (20°). In the former case the median error is $0.8\,\mathrm{m}$ with a standard deviation of $4\,\mathrm{cm}$, while in the latter the median error is $3.7\,\mathrm{m}$ with a standard deviation of $0.55\,\mathrm{m}$. Indeed, progressively shielding the antenna decreases the number of GNSS satellites in direct visibility, making the multi-path contribution predominant. The GNSS module receives signals from a constant number of approximately 30 satellites throughout the measurements, but shielding the antenna from the top allows the signal to reach the GNSS receiver only through ground reflections, thus decreasing the measurement accuracy.

Conclusion: The antenna shielding due to the train cab may have a significant impact on the positioning performance, depending on the train cab structure. Therefore, in order to maximize positioning accuracy, the GNSS antenna should be placed on the train roof.

V. Dynamic Tests on a Train

The on-train field tests were performed on the branch line between Formigine and Modena in Emilia-Romagna, Italy, over two days in October 2022. On this line, ETR103 trains manufactured by Alstom are operated by Trenitalia TPER. They have a maximum speed of $160\,\mathrm{km/h}$, although line speed on the line tested does not exceed $80\,\mathrm{km/h}$ and is generally no more than $60\,\mathrm{km/h}$. The line is electrified using $3\,\mathrm{kV}$ DC overhead line. It passes through a variety of GNSS and cellular environments, with sections of open sky view and sections with many buildings directly on both sides of the line which heavily limit the sky view. Cellular coverage is intermittent throughout. The line is mostly single track, with double-track passing loops at Modena Piazza Manzoni and Formigine stations, as well as multiple tracks in Modena station itself.

Two identical sensor nodes were used, with two different antennas. The antennas were placed in the rear cab of the train, and moved to the opposite cab at the end of each trip. The first sensor node was connected to a TOPGNSS TOP106 antenna L1/L2 multi-band antenna placed underneath

(a) (b)

Fig. 5. Dynamic tests: Sensor node antenna measurement setup for Sensor Node 1 (a) and Sensor Node 2 (b)

the rear windscreen of the train, on a flexible tripod fixed using adhesive putty and facing upwards. The setup can be seen in Fig. 5a (note that the other antennas in the background are from an unrelated experiment). The second sensor node used a smaller magnetic mount ANN-MB-00 L1/L2 dual band antenna which was affixed to the outside of the train above the window, approximately $2\,\mathrm{m}$ above the floor height of the train and approximately $1.4\,\mathrm{m}$ to the left of the left running rail, using adhesive putty, since the aluminum body shell of the train is not magnetic. This is shown in Fig. 5b. For the RTK corrections, a custom base station was set up by Sadel in Modena, Italy exposing the RTCM data produced by a ZED F9P module configured as an RTK base station via a raw TCP socket. The NTRIP protocol was not used for these tests.

A useful metric to evaluate the performance of the GNSS localization is to calculate the error between the GNSS point recorded by the ZED-F9P module and the actual location of the train and to compare this to the accuracy reported in the `hAcc` field of the `UBX-NAV-PVT` message by the GNSS module. However, on a moving train, this is challenging, particularly since the maps of the line available are of limited precision. Nevertheless, this was achieved as follows. A ground truth of the line was extracted from OpenStreetMap in GeoJSON format. Both the GeoJSON file and the data extracted from the ZED module are projected from the global WGS84 (EPSG: 4326) Coordinate Reference System to the locally flat UTM 32 projection (EPSG:25832) using the `PyProj` library [34]. The minimum distance between each GNSS point and the ground truth is then calculated using the `shapely` library [35]. While useful, this approach still has several limitations. The sensor node is not located precisely above the track axis, but rather has a certain offset, which is reported as an error. Moreover this metric calculates the distances from the position reported by the GNSS module to the track axis, but not to the actual position of the train, particularly in the longitudinal direction along the track. Nevertheless, this metric is still useful for assessing localization performance.

A. Results

Fig. 6 shows the number of satellites detected by each sensor node during the same trip between Formigine and Modena. Arrival and departure times at each station, are indicated in green and red respectively, while the connectivity of the cellular module and RTCM correction messages is indicated in

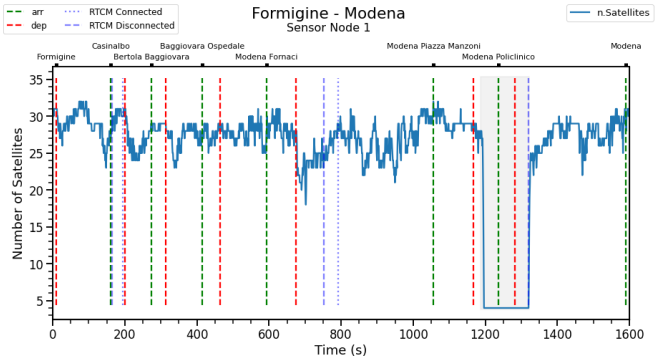

(a)

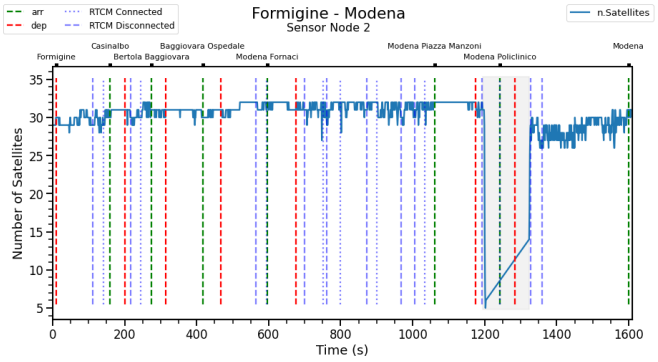

(b)

Fig. 6. Number of Satellites received by Sensor Node 1 (a) and Sensor Node 2 (b) on a measurement run between Formigine and Modena

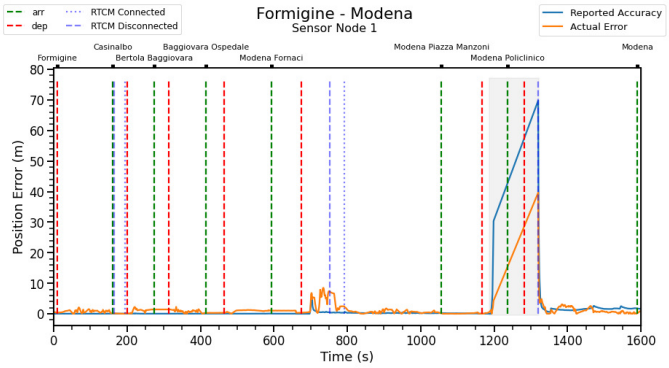

Fig. 7. Position Error reported by the GNSS module and the actual error relative to the ground truth for the entire measurement run of Sensor Node 1 between Formigine and Modena, including cellular connectivity status

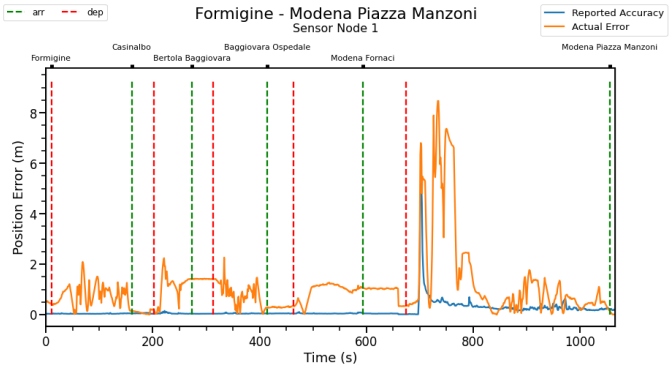

(a)

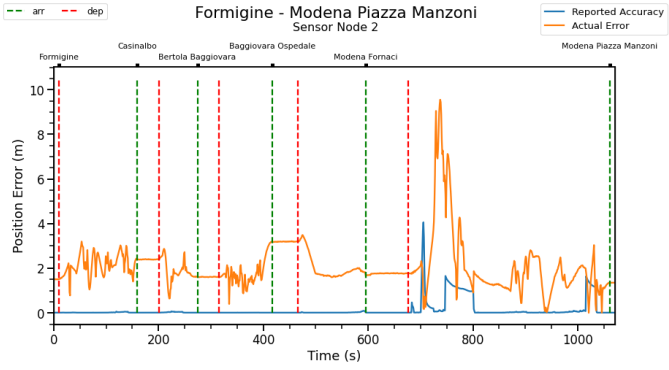

(b)

Fig. 8. Position Error reported by the GNSS module and the actual error relative to the ground truth, without the tunnel section, for Sensor Node 1 (a) and Sensor Node 2 (b)

blue. The approximate location of the tunnel between Modena Piazza Manzoni and Modena stations is indicated in gray.

It is clear that both sensor nodes receive signals from a large number of satellites. However, while the number of satellites is relatively consistent throughout the line for Sensor Node 2 (with the small antenna outside), ranging from 26 to 32, the number of satellites received by Sensor Node 1 is much more variable, with a minimum of 18 and a maximum of 32. The exception to this is inside the tunnel, where no more valid GNSS points are received by both sensor nodes shortly after the train enters.

The effect of the tunnel can also be seen clearly in Fig. 7. The accuracy reported in the `hAcc` field of the `UBX-NAV-PVT` message is shown in blue, while the distance to the ground truth is shown in orange. Note that while an accuracy is reported by the GNSS module, the `invalidLlh` flag of the `UBX-NAV-PVT` message is set throughout the tunnel, meaning the reported data is not considered to be valid.

The relationship between the reported accuracy and the actual error to the ground truth is shown in more detail for both sensor nodes between Formigine and Modena Piazza Manzoni (before the tunnel) in Fig. 8. Moreover, statistics are given in Table II. It is clear that there is not necessarily a direct relationship between the accuracy reported by the GNSS module (which is $1\,\mathrm{cm}$ almost throughout), and the actual accuracy as measured relative to the ground truth, which is significantly worse than reported by the GNSS module. Nevertheless the actual accuracy is within $2\,\mathrm{m}$ for most of the line, apart from shortly after departure from Modena Fornaci station. Although the raw numbers suggest otherwise, Sensor Node 2 appears to provide a more accurate position, once its offset to the track center-line (of approximately $2\,\mathrm{m}$) is taken into account. Sensor Node 1 is located almost directly above the track center-line and therefore is significantly less accurate in comparison. This is confirmed by the standard deviation σ which is noticeably smaller for Sensor Node 2.

On both error plots in Fig. 8, there are several peaks shortly after departing Modena Fornaci station. Two satellite map

TABLE II
POSITION ERROR SUMMARY STATISTICS

Metrics		Reported Error	Actual Error
μ (m)	Sensor Node 1	0.163983	1.075075
	Sensor Node 2	0.128677	2.065174
σ (m)	Sensor Node 1	0.352838	1.324148
	Sensor Node 2	0.380484	1.123460

extracts of this section can be seen in Fig. 9, where the ground truth is indicated in yellow, Sensor Node 1 in blue and Sensor Node 2 in orange. These peaks appear two have two distinct causes. First, directly after leaving Modena Fornaci, the line passes through an underpass under a highway, as shown in Fig. 9a. This causes the reported accuracy to briefly decrease. This is also reflected in Fig. 6, where there is a decrease in the number of visible satellites, particularly for Sensor Node 1. It can be seen that the reported positions of the sensor nodes diverge from the path of the line, especially for Sensor Node 1. For Sensor Node 1, this reported error peak is synchronous with a peak in the actual error relative to the ground truth, as would be expected. In contrast, for Sensor Node 2, no such actual error peak is visible. The map in Fig. 9a also does not indicate a deviation for Sensor Node 2 at this stage.

A significantly larger peak in the actual error relative to the ground truth occurs shortly afterwards for both sensor nodes, but does not have a corresponding reported error peak. A closer look at the map, as shown in Fig. 9b suggests that rather than being caused by an incorrectly determined position, an error in the ground truth itself appears more likely. The orthophoto background indicates that the ground truth passes through several trees, while the sensor node measurements pass through an adjacent clearer area while following a far smoother curved path. Due to the relatively poor quality of the satellite orthophoto, it is difficult to fully identify the cause of the error, but given that neither the ground truth nor the satellite image offer sufficient accuracy guarantees. and that the exact origin of this data is unknown, it is not unreasonable to conclude that the GNSS measurements from the sensor nodes may in fact be significantly more accurate than the ground truth and error plot would suggest. A combination of factors is also likely.

For Sensor Node 2, another, flatter peak in the reported error occurs at around $t = 750$ s. This can likely be explained by this sensor node's intermittent connection to the RTCM server at this stage, as can be seen in Fig. 6b. No such peak is visible for Sensor Node 1, which also does not lose connectivity during this time period.

(a)

(b)

Fig. 9. Maps showing position error near Modena Fornaci in areas of interest under a highway overpass (a) and a region with potentially inaccurate ground truth (b). The ground truth is indicated in yellow, Sensor Node 1 in blue and Sensor Node 2 in orange

VI. CONCLUSION

This work evaluated the performance of GNSS and RTK in static and dynamic conditions. In static conditions, with clear sky view, centimeter accuracy is achievable using RTK, whereas in urban environments, multi-path has a notable impact on positioning accuracy, limiting or even worsening the precision achievable. In a static test with a grounded metal plate, we demonstrate under controlled conditions that GNSS accuracy decreases as sky view is obstructed, from 0.80 ± 0.04 m in the least shielded case, to 3.70 ± 0.55 m in the most shielded case, with a constant number of GNSS satellite signals received throughout.

Furthermore, we performed dynamic tests on a railway line between Formigine and Modena in Emilia-Romagna, Italy in which GNSS, RTK, and IMU data was collected in several measurement runs using a custom sensor node. In this work, the horizontal accuracy and satellite coverage of the GNSS data with RTK is evaluated, and compared to a ground truth derived from publicly available data. The self-reported accuracy of the GNSS module with RTK enabled is within $16\,\mathrm{cm}$ on average, when not obstructed by long over-bridges or tunnels. The actual error when compared to the track center-line is much larger, but still within $1.3\,\mathrm{m}$ on average when antenna position is taken into account. However some of this error is likely to be caused by limited accuracy of the available ground truth track center-line.

The data sets for the dynamic tests will be open and freely available[1] for future work by the scientific community, addressing an acute lack of such data currently in the public domain. Our results are in line with other measurements in the literature [25] and reiterate that the self-reported accuracy cannot be relied upon in practice, meaning a sensor fusion approach with additional sensors is needed when GNSS is not available or has poor accuracy. We show that RTK is a promising approach for the railway environment, but also has severe limitations, and can even decrease the positioning

accuracy compared to GNSS alone under unfavorable conditions. The development of a novel sensor fusion algorithm to integrate the collected IMU data with GNSS and RTK will form the basis for our future work. Further investigation is also needed into how a reliable ground truth can be collected for the railway line so that real-time localization performance can be quantified more easily.

ACKNOWLEDGMENT

This work was partially supported by the Emilia-Romagna region under Project POR-FESR 2014-2020. Moreover, we would like to sincerely thank FER (Ferrovie Emilia Romagna) and Trenitalia Tper for their invaluable support during in-field tests.

REFERENCES

[1] J. Beugin, A. Filip, J. Marais, and M. Berbineau, "Galileo for railway operations: question about the positioning performances analogy with the RAMS requirements allocated to safety applications," *European Transport Research Review*, vol. 2, no. 2, pp. 93–102, 2010.

[2] W. Jiang, Y. Yu, K. Zong, B. Cai, C. Rizos, J. Wang, D. Liu, and W. Shangguan, "A seamless train positioning system using a LiDAR-aided hybrid integration methodology," *IEEE Transactions on Vehicular Technology*, vol. 70, no. 7, pp. 6371–6384, 2021.

[3] J. Pachl, *Railway operation and control*. VTD Rail Publishing, 2002.

[4] V. Quiñones, A. Águila, and I. Cordero, "GNSS4Rail simulation tool. supporting Virtual Balise (VB) location for GNSS based railway operations," in *2021 International Conference on Electrical, Computer, Communications and Mechatronics Engineering (ICECCME)*. IEEE, 2021, pp. 1–5.

[5] EUSPA, "Report on rail user needs and requirementsl," EUSPA, Tech. Rep., 2021. [Online]. Available: https://www.gsc-europa.eu/sites/default/files/sites/all/files/Report_on_User_Needs_and_Requirements_Rail.pdf

[6] P. Mayer, M. Magno, A. Berger, and L. Benini, "RTK-LoRa: High-Precision, Long-Range, and Energy-Efficient Localization for Mobile IoT Devices," *IEEE Transactions on Instrumentation and Measurement*, vol. 70, pp. 1–11, 2021.

[7] Y. Zhou, Q. Chen, and X. Niu, "Kinematic measurement of the railway track centerline position by GNSS/INS/odometer integration," *IEEE Access*, vol. 7, pp. 157 241–157 253, 2019.

[8] Y. Zhou, Q. Chen, R. Wang, G. Jia, and X. Niu, "Onboard train localization based on railway track irregularity matching," *IEEE Transactions on Instrumentation and Measurement*, vol. 71, pp. 1–13, 2022.

[9] A. Schütz, D. E. Sánchez-Morales, and T. Pany, "Precise positioning through a loosely-coupled sensor fusion of GNSS-RTK, INS and LiDAR for autonomous driving," in *2020 IEEE/ION Position, Location and Navigation Symposium (PLANS)*, 2020, pp. 219–225.

[10] EUSPA, "GNSS User Technology Report," EUSPA, Tech. Rep., 2020. [Online]. Available: https://www.euspa.europa.eu/simplecount_pdf/tracker?file=uploads/technology_report_2020.pdf

[11] J. Otegui, A. Bahillo, I. Lopetegi, and L. E. Díez, "Evaluation of experimental GNSS and 10-DOF MEMS IMU measurements for train positioning," *IEEE Transactions on Instrumentation and Measurement*, vol. 68, no. 1, pp. 269–279, 2018.

[12] EUSPA, "EUSPA EO and GNSS market report," EUSPA, Tech. Rep., 2022. [Online]. Available: https://www.euspa.europa.eu/sites/default/files/uploads/euspa_market_report_2022.pdf

[13] C. Amatetti, T. Polonelli, E. Masina, C. Moatti, D. Mikhaylov, D. Amato, A. Vanelli-Coralli, M. Magno, and L. Benini, "Towards the Future Generation of Railway Localization and Signaling Exploiting sub-meter RTK GNSS," in *2022 IEEE Sensors Applications Symposium (SAS)*. IEEE, 2022, pp. 1–6.

[14] D. Mikhaylov, "Future generation of highly precise real-time localization for railway applications," Master's thesis, ETH Zurich, 2022.

[15] E. Masina, "Future generation of railway localization and signaling exploiting sub-meter GNSS localization and 5G connectivity," Master's thesis, ETH Zurich, 2022.

[16] K.-W. Chiang, H.-W. Chang, Y.-H. Li, G.-J. Tsai, C.-L. Tseng, Y.-C. Tien, and P.-C. Hsu, "Assessment for INS/GNSS/odometer/barometer integration in loosely-coupled and tightly-coupled scheme in a GNSS-degraded environment," *IEEE Sensors Journal*, vol. 20, no. 6, pp. 3057–3069, 2019.

[17] S. A. Kazim, N. A. Tmazirte, and J. Marais, "Realistic position error models for GNSS simulation in railway environments," in *2020 European Navigation Conference (ENC)*. IEEE, 2020, pp. 1–9.

[18] M. Caamano, O. G. Crespillo, D. Gerbeth, and A. Grosch, "Detection of GNSS multipath with time-differenced code-minus-carrier for land-based applications," in *2020 European Navigation Conference (ENC)*. IEEE, 2020, pp. 1–12.

[19] P. Zabalegui, G. De Miguel, A. Pérez, J. Mendizabal, J. Goya, and I. Adin, "A review of the evolution of the integrity methods applied in GNSS," *IEEE Access*, vol. 8, pp. 45 813–45 824, 2020.

[20] Y. Zhang, D. Lu, B. Cai, and J. Liu, "3D digital track map-based GNSS NLOS signal analytical identification method," in *2021 International Conference on Electromagnetics in Advanced Applications (ICEAA)*. IEEE, 2021, pp. 313–318.

[21] S. Jiang, D. Lu, and B. Cai, "GNSS NLOS signal modeling and quantification method in railway urban canyon environment," in *2019 IEEE Intelligent Vehicles Symposium (IV)*. IEEE, 2019, pp. 1268–1273.

[22] C. Stallo, A. Neri, P. Salvatori, R. Capua, and F. Rispoli, "GNSS integrity monitoring for rail applications: Two-tiers method," *IEEE Transactions on Aerospace and Electronic Systems*, vol. 55, no. 4, pp. 1850–1863, 2018.

[23] T. Daoust, F. Pomerleau, and T. D. Barfoot, "Light at the end of the tunnel: High-speed LiDAR-Based train localization in challenging underground environments," in *2016 13th Conference on Computer and Robot Vision (CRV)*, 2016, pp. 93–100.

[24] L. Peng, S. Zheng, P. Li, Y. Wang, and Q. Zhong, "A comprehensive detection system for track geometry using fused vision and inertia," *IEEE Transactions on Instrumentation and Measurement*, vol. 70, pp. 1–15, 2021.

[25] J. Otegui, A. Bahillo, I. Lopetegi, and L. E. Díez, "A Survey of Train Positioning Solutions," *IEEE Sensors Journal*, vol. 17, no. 20, pp. 6788–6797, 2017.

[26] J. Beugin, C. Legrand, J. Marais, M. Berbineau, and E.-M. El-Koursi, "Safety appraisal of GNSS-based localization systems used in train spacing control," *IEEE Access*, vol. 6, pp. 9898–9916, 2018.

[27] J. Otegui, A. Bahillo, I. Lopetegi, and L. E. Díez, "Simulation framework for testing train navigation algorithms based on 9-DOF-IMU and tachometers," *IEEE Transactions on Instrumentation and Measurement*, vol. 69, no. 7, pp. 5260–5273, 2020.

[28] S. Bisnath, "Relative positioning and real-time kinematic (RTK)," *Position, Navigation, and Timing Technologies in the 21st Century: Integrated Satellite Navigation, Sensor Systems, and Civil Applications*, vol. 1, pp. 481–502, 2020.

[29] I. Um, S. Park, S. Oh, and H. Kim, "Analyzing location accuracy of unmanned vehicle according to RTCM message frequency of RTK-GPS," in *2019 25th Asia-Pacific Conference on Communications (APCC)*. IEEE, 2019, pp. 326–330.

[30] S. Mahato, A. Santra, S. Dan, P. Rakshit, P. Banerjee, and A. Bose, "Preliminary results on the performance of cost-effective GNSS receivers for RTK," in *2019 URSI Asia-Pacific Radio Science Conference (AP-RASC)*. IEEE, 2019, pp. 1–4.

[31] M. Specht, C. Specht, A. Stateczny, P. Burdziakowski, P. Dabrowski, and O. Lewicka, "Study on the positioning accuracy of the GNSS/INS system supported by the RTK receiver for railway measurements," *Energies*, vol. 15, no. 11, p. 4094, 2022.

[32] C. Moore, "Geofencing trial begins as network rail continues track worker safety drive," *New Civil Engineer*, 2022. [Online]. Available: https://www.newcivilengineer.com/latest/geofencing-trial-begins-as-network-rail-continues-track-worker-safety-drive-19-10-2022/

[33] E. Kaplan and C. Hegarty, *Understanding GPS: Principles and Applications*, ser. Artech House mobile communications. Artech House, 2006.

[34] A. D. Snow, J. Whitaker, M. Cochran *et al.*, "pyproj4/pyproj: 3.4.0 release," Sep. 2022. [Online]. Available: https://doi.org/10.5281/zenodo.7065964

[35] S. Gillies, C. van der Wel, J. Van den Bossche, M. W. Taves, J. Arnott, B. C. Ward *et al.*, "Shapely." [Online]. Available: https://github.com/shapely/shapely